

# Pilot testing of a novel integrated Multi Effect Distillation - Absorber compressor (MED-AB) technology for high performance seawater desalination

Shahzada Aly<sup>a</sup>, Jasir Jawad<sup>a</sup>, Husnain Manzoor<sup>a</sup>, Simjo Simson<sup>a</sup>, Jenny Lawler<sup>a</sup>, Abdel Nasser Mabrouk<sup>a, b, \*</sup>

<sup>a</sup> Qatar Environment and Energy Research Institute, Hamad Bin Khalifa University, Qatar Foundation, 34110 Doha, Qatar

<sup>b</sup> College of Science and Engineering, Hamad Bin Khalifa University, Doha, Qatar

## HIGHLIGHTS

- Novel design of an integrated MED-AB process
- Installation of 25 m<sup>3</sup>/day pilot plant based novel design
- Simulation and pilot testing validate the new design
- 60% lower in specific energy consumption (MED-AB = 4.8 kWh/m<sup>3</sup>)
- 20% reduction in the unit water cost (MED-AB = 0.455 \$/m<sup>3</sup>)

## GRAPHICAL ABSTRACT

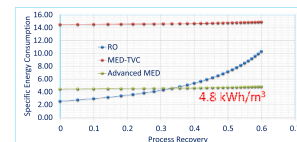
### Advanced MED-AB Technology for Seawater Desalination

#### Installation of an advanced MED-AB pilot plant

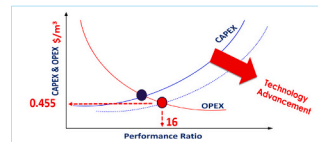
- Demonstrate the new concept 25 m<sup>3</sup>/day capacity
- Verify the new design concept,
- Validate the mathematical model,
- 60 % lower in the specific energy consumption,
- 20 % lower in the unit water cost.



Advanced MED pilot plant for desalination



QATAR ENVIRONMENT AND ENERGY RESEARCH INSTITUTE Dr. Abdel Nasser Mabrouk



## ARTICLE INFO

### Keywords:

Thermal Desalination  
Multi-Effect Distillation (MED)  
Absorber Generator (AB)  
Energy Recovery  
Techno-economics  
Pilot Plant

## ABSTRACT

This work presents a novel integration of Multi Effect Distillation with Absorption compressor (MED-AB) to reduce the energy consumption and unit water cost. The MED-AB pilot plant has been installed with a nominal capacity of 25 m<sup>3</sup>/day to validate the concept under a seawater salinity of 57,500 ppm (West of Qatar). Both pilot testing and the simulation results confirm the features of the novel design of the MED-AB process. Simulation of a commercial evaporator of 15 MIGD capacity showed that the specific energy consumption of the proposed MED-AB is calculated as 4.8 kWh/m<sup>3</sup>, which is 60% lower than the existing MED-TVC plant (13 kWh/m<sup>3</sup>). Compared to the traditional MED-TVC, the seawater feed and pumping power of MED-AB process is lower by 70% and 55%,

**Abbreviations:** A, Surface area (m<sup>2</sup>); AB, Absorber Generator system; ABHP, Absorption Heat Pumps; ACHP, Absorption-Compression Heat Pump; ADHP, Adsorption Heat Pumps; CAPEX, Capital Expenditure; CCGT, Combined Cycle Gas Turbine; CFD, Computational Fluid Dynamics; COP, Coefficient of Performance; FF, Fouling Factor; GOR, Gained Output Ratio; LiBr-H<sub>2</sub>O, Lithium Bromide Solution; MED, Multi-Effect Distillation; MED-AB, Multi Effect Distillation with Absorption Compressor; MIGD, Million Imperial Gallons per Day; MSF, Multi-Stage Flash; MVC, Mechanical Vapor Compression; NCGs, Non-Condensable Gases; OPEX, Operating Expenditure; PLC, Programmable Logic Controller; PR, Performance Ratio; RO, Reverse Osmosis; SEC, Specific Energy Consumption; SCADA, Supervisory Control and Data Acquisition; SR, Salt Rejection; TBT, Top Brine Temperature; TDS, Total Dissolved Solids; TVC, Thermal Vapor Compression; VSP, Visual Simulation Program; VCR, Vapor Compression Refrigeration; VCHP, Vapor Compression Heat Pump.

\* Corresponding author at: Qatar Environment and Energy Research Institute, Hamad Bin Khalifa University, Qatar Foundation, 34110 Doha, Qatar.

E-mail address: [aaboukhlewa@hbku.edu.qa](mailto:aaboukhlewa@hbku.edu.qa) (A.N. Mabrouk).

<https://doi.org/10.1016/j.desal.2021.115388>

Received 24 July 2021; Received in revised form 8 September 2021; Accepted 4 October 2021

Available online 9 October 2021

0011-9164/© 2021 The Authors. Published by Elsevier B.V. This is an open access article under the CC BY license (<http://creativecommons.org/licenses/by/4.0/>).

respectively. The results confirm the minimization of the environmental impact of dumping thermal energy back into the sea and reduce the plant's capital investment, covering feed pumps size and the intake/outfall civil work. The levelized unit water cost of the MED-AB is calculated as 0.46 \$/m<sup>3</sup>, which is 22% lower than that of a conventional MED-TVC desalination plant. The novel MED-AB technology would create a potential solution for the industrial applications of high salinity byproduct and solar desalination.

## 1. Introduction

Seawater desalination and water purification is a sustainable solution in arid countries lacking natural potable water, especially those are experiencing an immense growth in population, economy, and industrial activities. The State of Qatar has one of the highest water consumptions per capita in the world, reaching nearly 500 l per day [1]. Therefore, the increase in population and water use intensity, coupled with the continued shortage of natural drinking water in the country, will require a rapid increase in the desalination capacity. The desalination technology provides 97% of the municipality produced water in Qatar. Currently, the desalination technology generates 539 million imperial gallons per day (MIGD) in which thermal desalination (MSF and MED) generates 65% while the remainder (35%) is generated by Reverse Osmosis technology (RO) as shown in Fig. 1 [2].

Due to the site-specific of Gulf seawater, the selection of the right desalination technology usually is frequently subjected to the compromise between the thermal and membrane desalination. There are many factors such as energy efficiency, reliability under harsh conditions, and lower unit costs. Due to the characteristics of harsh Gulf seawater (high temperature reaching more than 37 °C in summer, residuals of boron, high TDS and bromides, and the severe fluctuations in the seawater intake quality), the RO membrane technology facing a true operational challenges. Accordingly, thermal desalination is still considered a reliable technology, however, its typical specific energy consumption showed that a significant potential for improvement compared with the thermodynamic limits of separation of 1.0 kWh/m<sup>3</sup>.

The least exergy required for saltwater separation using membrane and thermal concepts, under the same process recovery ratio, showed the same value of specific energy consumption which should be identical in nature [3]. Currently, the RO technology shows a lower specific energy consumption due to the use of an efficient energy recovery system. However, the thermal desalination processes have not yet deployed an efficient thermal energy recovery system. Till recent times, most of the thermal desalination R&D focus has been evolving on increasing the unit evaporator size (20 MIGD per unit MSF evaporator and 15 MIGD per unit MED evaporator) to reduce the capital cost. However, there has been little research attention paid to the development of an efficient energy recovery system to reduce thermal energy consumption.

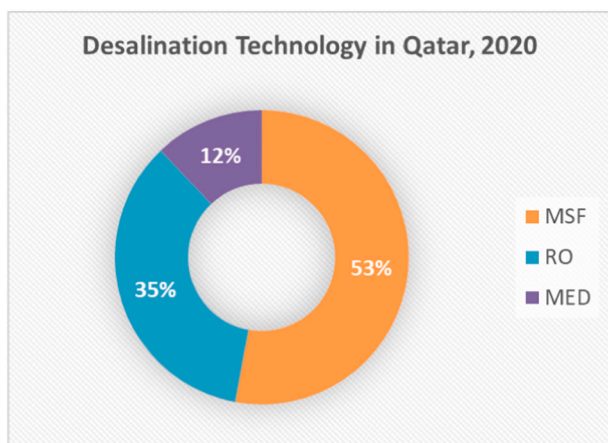


Fig. 1. Market share of desalination technology in Qatar, 2020.

The thermal desalination technologies can be much cheaper if abundant waste heat is available [4–8]. Therefore, thermal desalination units are often installed in the vicinity of fuel-based power plants, often termed as cogeneration in the industry. Comparison between MSF, MED and RO has shown that the specific energy consumption of all technologies, regardless of the type, is less when integrated with higher efficiency combined cycle gas turbine power plant. However, thermal desalination gets more advantage due to using a lower exergy of the low-pressure steam. The high Performance Ratio (16–19) MED could compete with RO, particularly at high salinity water feed [5,6].

Analogous to the energy recovery system implemented in RO plant, thermal desalination processes are also often combined with the thermal versions of energy recovery systems. The common combinations with thermal desalination are heat pumps. The most common heat pumps are ejector heat pumps or thermal vapor compression (TVC), absorption heat pumps (ABHP) and adsorption heat pumps (ADHP). Whatever the feasible choice under given conditions may be, the ultimate goal is to enhance the GOR and water production of the stand-alone thermal desalination unit for the same amount of thermal energy consumption.

Multi effect desalination with thermal vapor compression 'MED-TVC' of various configurations is a dominating technology in the desalination market [9–12]. In MED-TVC configuration, usually motive steam at 3 bar & 140 °C causes entrainment of vapor at lower pressure from middle effect to raise its pressure and use as a heating steam in the first effect. So, with TVC, steam consumption is lower than simple MED system resulting in higher gain output ratio (GOR), which is defined by the ratio of mass flowrate of the distillate production and consumed motive steam flow rate. However, the TVC entrainment capacity is constrained with both motive pressure ratio and the compression ratio. As long as the compression ratio increases, the expansion pressure ratio will increase as well. This means that to handle a big quantity of vapor from the last effect, a substantial amount of motive steam is required, typically around 20 bar. However, this high-pressure steam is relatively expensive compared to the low-pressure steam at 3 bar.

A theoretical model of low-temperature MED coupled with LiBr-H<sub>2</sub>O ABHP has been developed by Wang and Lior [13] under typical motive steam pressure of 1.2–5 bars. In this system, heating steam required for MED comes from three sources: (a) from the solution boiled off in the generator, (b) from the evaporated condensate from the first effect in the absorber and (c) from flashing of a part of the motive steam condensate. The combined system gives a 60 to 78% water production gain over a stand-alone Low Temperature Multi Effect Evaporation (LT-MEE) unit run by the same heat source conditions [13]. The economic performance comparison showed that the MED-ABHP has better economic performance than MED-TVC when the steam cost is greater than 1.44 \$/ton. However, the proposed system still used down condenser to dump thermal energy back to the sea. Also, no practical implementation of the proposed system was demonstrated by the authors.

An absorption cycle and MED of 20 effects was theoretically analyzed [14]. The desalination system's top brine temperature (TBT) was 63 °C, while the last effect temperature was 6 °C as a results the GOR is calculated as 14.8. The proposed system can also provide as a byproduct cooling capacity. However, the author did not consider the expensive cost of the high-quality motive steam to drive as such a large operating range of 57 °C, compared to the operating range of the traditional MED-TVC, which is mostly 25 °C.

Esfahani et al. [15] proposed a system that combines Li-Br solution based ABHP with a 6-cell MED, where the MED acts as a sub-system of

the larger vapor-compression refrigeration (VCR) system. The MED unit replaces the condenser part of the VCR to recover its waste energy. The energy and economic analysis showed that the electrical and thermal energy demand can be reduced by 57% and 5% respectively, while COP and GOR can be enhanced up to 57% and 5%. The reason for sharp decrease in electrical power consumption is due to less pressure ratio needed by the compressor in the proposed combined system as opposed to the standalone VCR system.

Practical demonstration of the feasibility of first double effect LiBr-H<sub>2</sub>O ABHP prototype was done at Plataforma Solar de Almería (CIEMAT, Spain [16]). In this system there is no direct use of the vapor generated in the last effect. The hot water from ABHP is used as heating source of the first effect. The ABHP, coupled with compound parabolic concentrator (CPC) solar collector field was designed to provide hot water at 66.5 °C to the first effect of the MED [17]. The absorber and generators along with their condenser and evaporator had a cooling capacity with a coefficient of performance (COP) of 2.22 at 100% load, i. e., energy received by hot water at 180 °C coming from CPC or the backup gas-fired boiler. Later it was shown that using ABHP, the collector area of a solar based MED plant can be almost halved [17]. A double effect LiBr-H<sub>2</sub>O ABHP combined with a 9-effect LT-MED was shown to have a potential GOR of 17, as compared to a same size MED-TVC having a GOR of 11. This, and some other studies, shows that ABHP are more efficient than TVC [18].

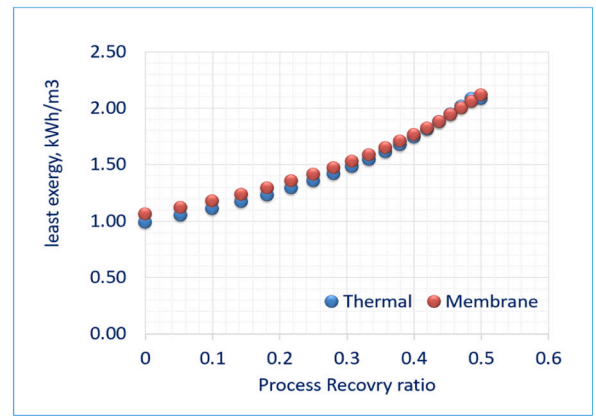
Rostamzadeh et al. [19] proposed integrating MED with ABHP and VCHP independently. The absorbent proposed for ABHP was ammonia-water solution, while the refrigerant for the VCHP was considered to be the vapor from last effect of the MED unit. Both proposed systems were compared to conventional mechanical vapor compression (MVC), i.e., MED-MVC setup. The comparison suggested that the MED-MVC has the lowest water production rate, while that for MED-VCHP and MED-ABHP were 6.7% and 110.3% higher. Therefore, according to the computational analysis of their configuration designs, MED-VCHP results in highest thermodynamic and exergy related gains, while MED-ABHP ranks lowest amongst the three systems.

The thermodynamic analysis presented in the supplementary material A revealed that the least exergy for thermal and membrane process are equal as shown in Fig. 2 (a). However, for commercial MED-TVC (GOR = 8) and RO plants, there is a gap between in the specific energy consumption as shown in Fig. 2 (b). This gap is mainly due to the energy recovery system in RO, which is highly efficient than that used in thermal (TVC). Also, thermodynamic analysis presented in the supplementary material A indicated that as long as the performance ratio of the MED technology increases, the specific energy consumption eventually decreases, as shown in Fig. 3 (a), calculated using Eq. (1). On the other hand, while the performance ratio of MED increases, the heat transfer area increases too, as shown in Fig. 3 (b), calculated using Eq. (2). This situation motivated us to develop an efficient energy recovery system for MED technology to replace current TVC and eliminate the down condenser.

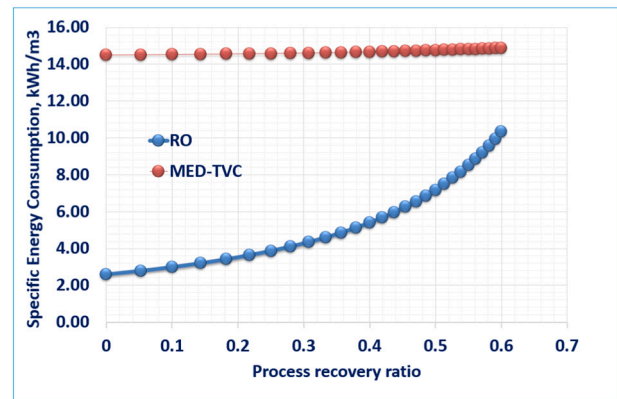
$$SEC_{conventional} = \frac{\lambda N (\delta + \Delta T_{app} + \Delta T_{loss})}{PR (T_0 + N (\delta + \Delta T_{app} + \Delta T_{loss}))} \quad (1)$$

$$\frac{A}{M_d} = \frac{N \lambda_d}{PR \times U (\Delta T_{stage} - (\delta + \varepsilon))} \quad (2)$$

In this work, we aim to present an integration of novel Multi Effect Distillation with Absorption compressor (MED-AB) process to reduce the energy consumption and unit water cost based on innovative ideas [20,21]. A modular design of MED-AB pilot plant has been installed with a nominal capacity of 25 m<sup>3</sup>/day to validate the concept under a seawater salinity of 57,500 ppm (West of Qatar), at the top brine temperature of 65 °C. A Visual Simulation Program (VSP) code [22] has been developed and validated using the installed MED-AB pilot plant. The VSP has then been utilized to simulate the commercial large-scale



(a)



(b)

Fig. 2. Least and typical exergy of the separation process.

MED-TVC unit evaporator to be compared with the present invention MED-AB in terms of performance ratio, heat transfer area and specific energy consumption. The VSP has been used to perform technoeconomic analysis of commercial plant based novel MED-AB process and compared with the conventional design.

## 2. Description of the MED-AB pilot plant

As shown in Fig. 4, the pilot plant has been installed on the coast of Dukhan sea, which is in the northwest of Qatar. This site is a bay in between Qatar and Saudi Arabia and has one of the highest sea water concentrations found around the globe. It has an average salinity of 57,500 ppm, which is high when compared to average seawater salinity of the world oceans (35,000 ppm). The novel desalination system is composed of two main units. One is the multi-effect distillation (MED) unit, and the other is absorber generator (AB) vapor compression unit. Due to the modular design of the pilot plant, it can be operated independently in two modes. First, as a standalone MED, referred to as 'EVAP' mode and second, in integration with the MED-AB, referred to as 'FULL' mode in this work. Fig. 5 shows the block flow diagram of the MED-AB desalination process (patent pending [20,21]).

### 2.1. Description of the MED 'EVAP' mode

Here we only present a summary of the MED unit, as the novel design and working of it has already been explained in detail in the earlier works of the authors [2]. As shown in Fig. 5, the MED unit consists mainly of three cells and a condenser. Each cell has a single-pass tube bundle design, where each bundle contains 660 tubes in total, in a square-pitch distribution. Whereas, the condenser has a three-pass

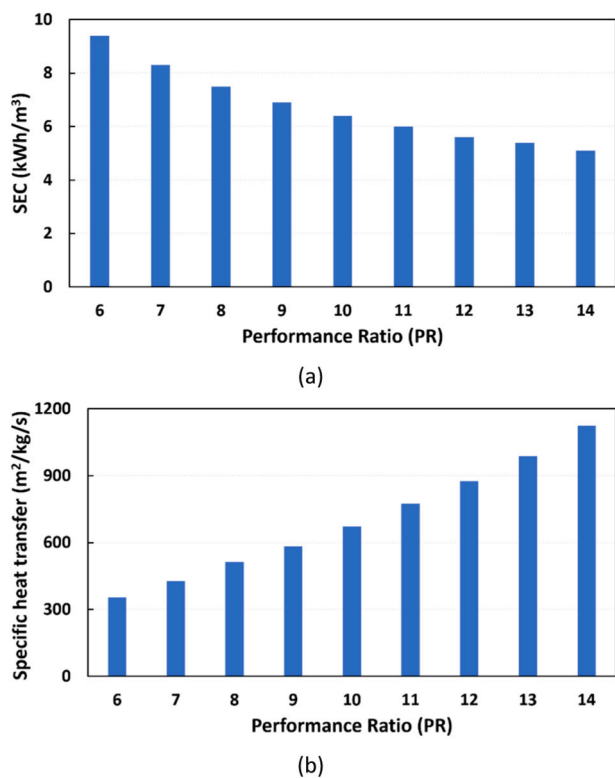


Fig. 3. (a) SEC vs. performance ratio (PR) and (b) heat transfer vs. performance ratio (PR).

design, with 225 tubes per pass (625 in total). The novel design of MED works on the same working principles of a standard MED desalination unit. When operating independently in MED 'EVAP' mode, as shown in Fig. 5, the tube bundle of cell 1 is fed steam from an electrical boiler

(stream 20). The shell side of cell 1, cell 2 and cell 3 receives the seawater feed (in form of falling film) directly from Dukhan sea (stream 9). Part of this feed is used to condense steam from the last cell going into the condenser and discharged back into the sea as a cooling reject (10). The seawater feed going into the evaporator cells is preheated using two heat exchangers: one on the brine discharge line (stream 18) and the other on the distillate discharge line (stream 19). The stream 18 and stream 19 flow proportions are controlled by the SCADA algorithm, which ensures that total vapor condensation occurs inside the condenser by continuously monitoring the vapor pressure inside the condenser. The distillate produced from cell 1 is returned back to the electrical boiler (stream 21 to 17), while the distillate produced from cell 2, cell 3 and condenser is sent in parallel to the distillate collection tank (stream 12). Similarly, the brine from each cell is sent to the next cell in series and finally the cumulative brine of all three cells is discharged to the sea (stream 11), after proper treatment. The series configuration of brine is to promote flashing and increase the overall distillate production. To periodically remove the non-condensable gases (NCGs) produced during the operation, a water ejector based vacuum system is used. The water ejector is also used to create initial vacuum of the entire system, whereas a vacuum oil pump is used for making a deeper vacuum to initiate the process. Once the system starts receiving steam from the boiler and the operation begins, then the thermodynamics itself naturally controls the pressure and temperature distributions within each cell.

## 2.2. Description of the MED-AB 'FULL' mode

The absorber generator (AB) vapor compression unit here is basically a heat pump, but without condenser and evaporator modules. The absorber receives vapor at a lower pressure and the generator produces steam at a higher pressure, thus mimicking a compressor. The carrier liquid for the AB unit in this system is LiBr-Water solution. Both, absorber and generator are shell and tube heat exchangers with a sieve tray to facilitate the falling film absorption/desorption process. The shell is kept under vacuum pressure lower or equal to the vapor pressure of the last cell 3 of the MED evaporator.

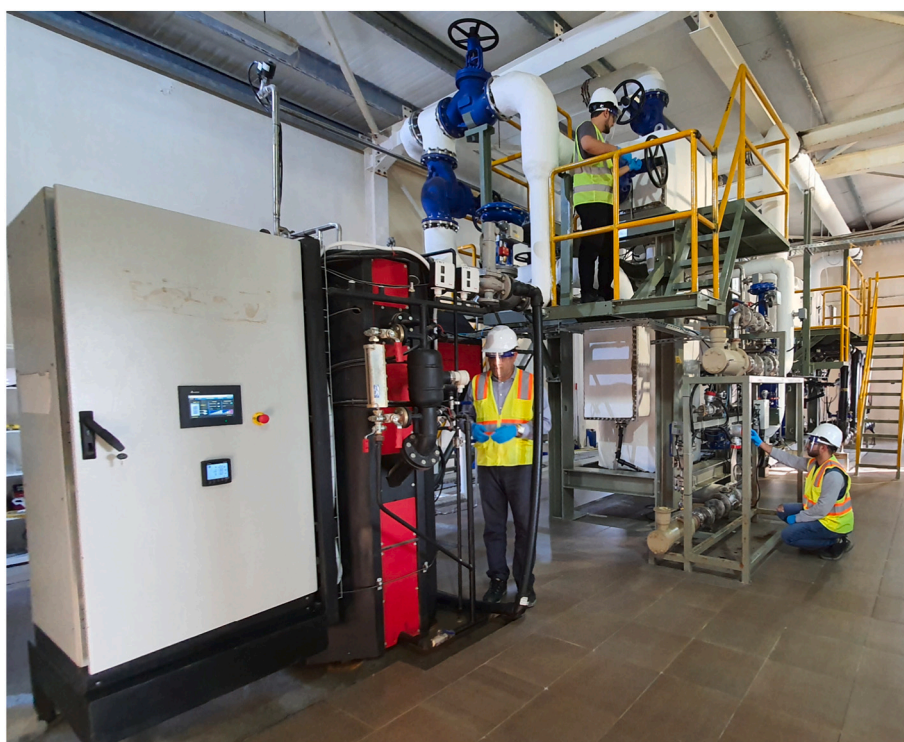


Fig. 4. Advanced MED-AB pilot plant at Dukhan, Qatar.

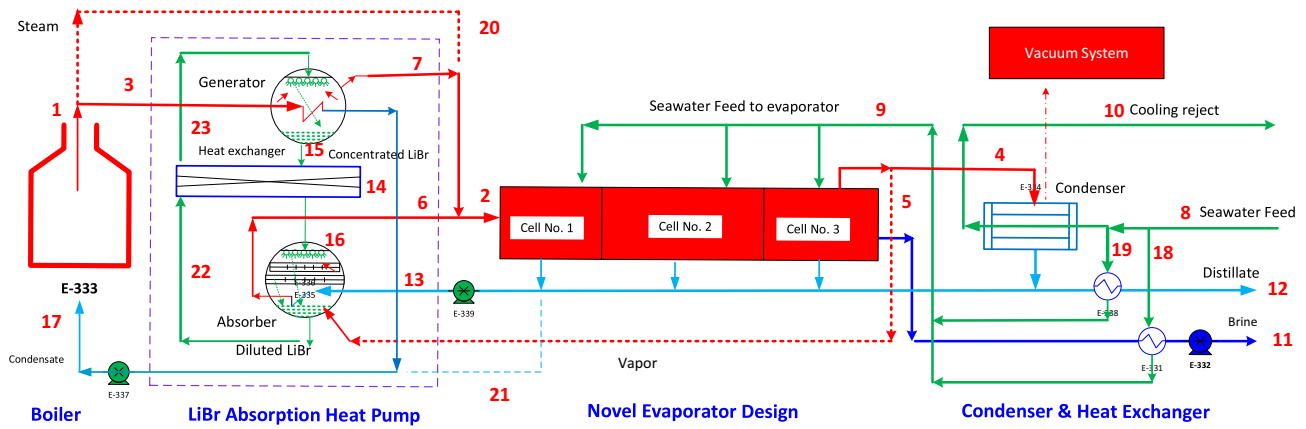


Fig. 5. Block flow diagram of the MED (‘EVAP’ mode) desalination system [20].

As shown in Fig. 6, the concentrated LiBr-H<sub>2</sub>O solution is sprayed on a tray(s) in the shell side to enhance the absorption of the vapor into the sprayed LiBr solution. The LiBr solution becomes diluted by absorbing the vapor of the last cell (stream 5). The absorption process releases adequate energy (exothermic reaction) due to condensing the vapor. Pure water (from the distillate, stream 13) is circulated through tubes as a cooling water to absorb the released energy from absorption reaction taking place in the shell side. This energy can be used to generate additional amount of water vapor (inside the tubes) to be used as a heating steam (stream 6) to the first cell. When the absorber receives vapor, it absorbs it and becomes a weak solution.

The diluted LiBr-H<sub>2</sub>O solution, stream No. 22, exchanges heat with concentrated solution, stream No. 15, through heat exchanger before entering the generator. While the motive steam, stream No. 3, flows inside the tubes, the temperature of the LiBr-H<sub>2</sub>O solution increased to the saturation conditions and results in evaporating the same amount of water vapor absorbed by the solution in the absorber. The generated vapor from both the generator, and the absorber, stream No.2, is routed to the first cell (effect) of MED evaporator. Seawater feed, stream No. 9 is distributed in parallel and gets preheated through preheaters before is spraying at the outer tubes of each evaporator. Part of seawater feed is evaporated due to the gain of the latent heat energy of the heating steam condensate inside the evaporator tubes. The sum of the condensate from the heating steam in the first cell (effect) and the condensate of the successive effects forms the distillate product steam, stream No. 12. The concentrated brine leaving the MED evaporator is rejected back to the sea, stream No. 12.

### 3. Mathematical modeling

This section presents the mathematical model of the generator and absorber. However, the mathematical model of the evaporator is presented in [23].

#### 3.1. Generator

As shown in Fig. 7, for the generator, there are 2 input streams (vapor from boiler or low-pressure steam from back pressure turbine/condensed turbine or solar system, LiBr-H<sub>2</sub>O feed) and 3 outlet streams (Condensate, LiBr-H<sub>2</sub>O brine outlet, and the generated vapor). Each stream is defined with its properties such as pure water flow rate, salt flow rate, temperature, and pressure. The number of unknowns is identified accordingly, and the number of governing equations is presented as follows:

Water balance for Generator:

$$V_{n-1} + W_{f,n} = V_n + W_{b,n} + D_n \quad (3)$$

$$V_{n-1} = D_n \quad (4)$$

Salt balance for Generator:

$$S_{f,n} = S_{b,n} \quad (5)$$

Heat balance around Generator:

$$V_{n-1}h_{v,n-1} + (W_{f,n} + S_{f,n})h_{LiBr-H_2O,in} = V_n h_{v,n} + (W_{b,n} + S_{b,n})h_{b,nLiBr-H_2O,out} + D_n h_{d,n} \quad (6)$$

As shown in Fig. 7 (‘a’ and ‘b’), the vapor ( $V_{n-1}$ ) of the heating source

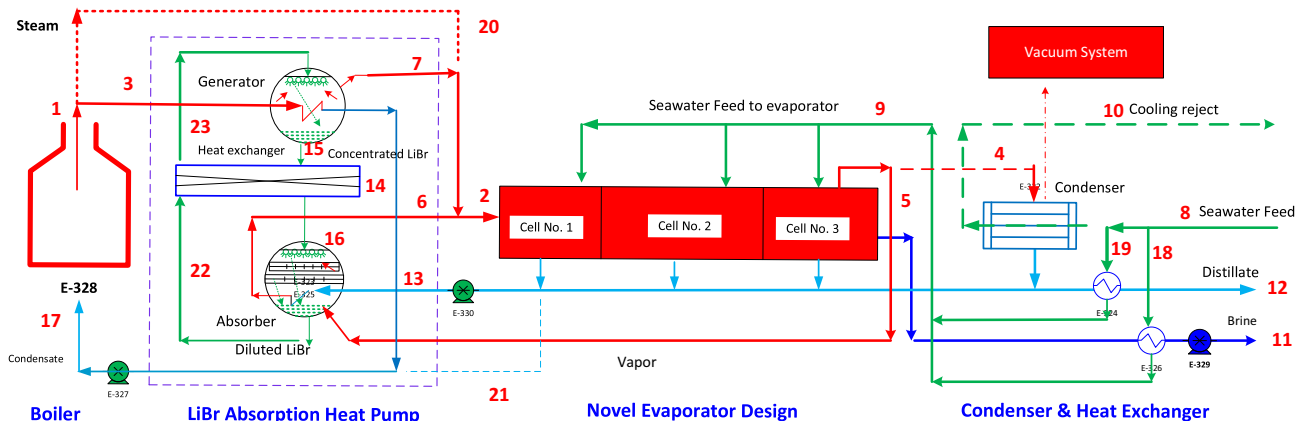


Fig. 6. Block flow diagram of the MED-AB (‘FULL’ mode) desalination system [21].

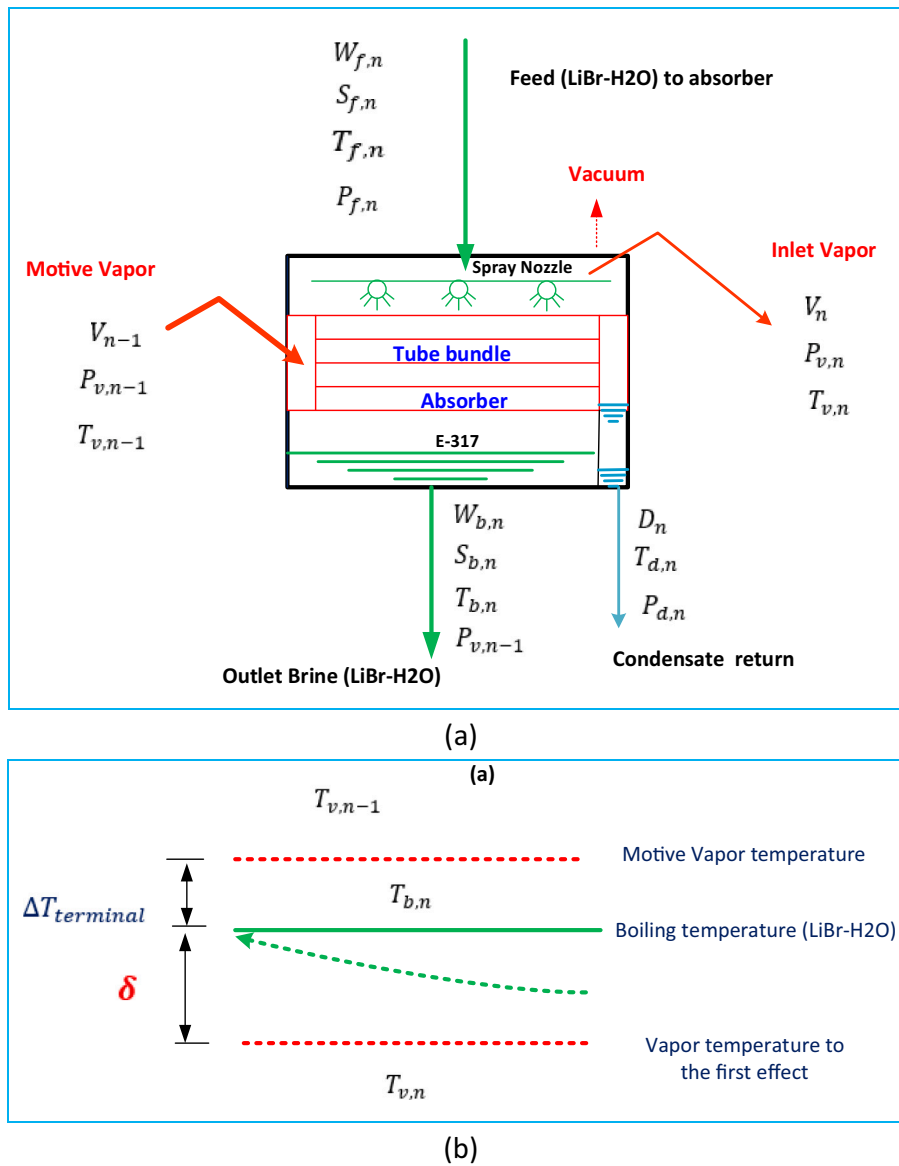


Fig. 7. Generator; (a) Control volume and (b) Temperature distribution.

is condensed inside the tubes of the generator, while the LiBr-H2O solution is sprayed on the outer side of the tubes. Due to steam condensation, heat is liberated to boil part of the falling film LiBr-H2O solution outside the tubes. The equilibrium state is determined at the shell pressure ( $P_{v,n}$ ) and the salinity of the LiBr-H2O solution at inlet ( $X_{inlet}$ ).

$$T_{boiling,Generator} = \varnothing(P_{v,n} \& X_{inlet}) \quad (7)$$

The temperature difference ( $\Delta T_{terminal}$ ) between the vapor ( $T_{v,n-1}$ ) and the LiBr-H2O fall ( $T_{b,n}$ ) is presented as:

$$\Delta T_{terminal} = T_{v,n-1} - T_{b,n} \quad (8)$$

The terminal temperature ( $\Delta T_{terminal}$ ) is determined from heating load, the overall heat transfer coefficient ( $U$ ) and the heating surface area ( $A$ ) of the tube bundle:

$$V_{n-1}h_{v,n-1} - D_n h_{d,n} = UA\Delta T_{terminal} \quad (9)$$

The overall heat transfer ( $U$ ) in Eq. (10) is calculated as:

$$U = 1 / \left( \frac{1}{h_i} + \frac{1}{h_o} + \frac{t}{k} + FF \right) \quad (10)$$

And heat transfer area ( $A$ ),

$$A = n\pi DL \quad (11)$$

where,  $n$ ,  $D$  and  $L$  are related to tube number, diameter, and length, respectively.

Also, the pressure of the generator ( $P_{boiling,Generator}$ ) is determined by the thermodynamic balance around the tube bundle.

$$P_{boiling,Generator} - P_{b,n} = 0 \quad (12)$$

$$P_{b,n} - P_{v,n} = \varnothing(\delta) \quad (13)$$

$$P_{v,n-1} = Specified \quad (14)$$

$$P_{v,n-1} - P_{D,n} = 0 \quad (15)$$

$$P_{f,n} - P_{b,n} = \varnothing(\Delta T_{subcooling}) \quad (16)$$

### 3.2. Absorber

As shown in Fig. 8, for the absorber, there are 3 input streams (vapor

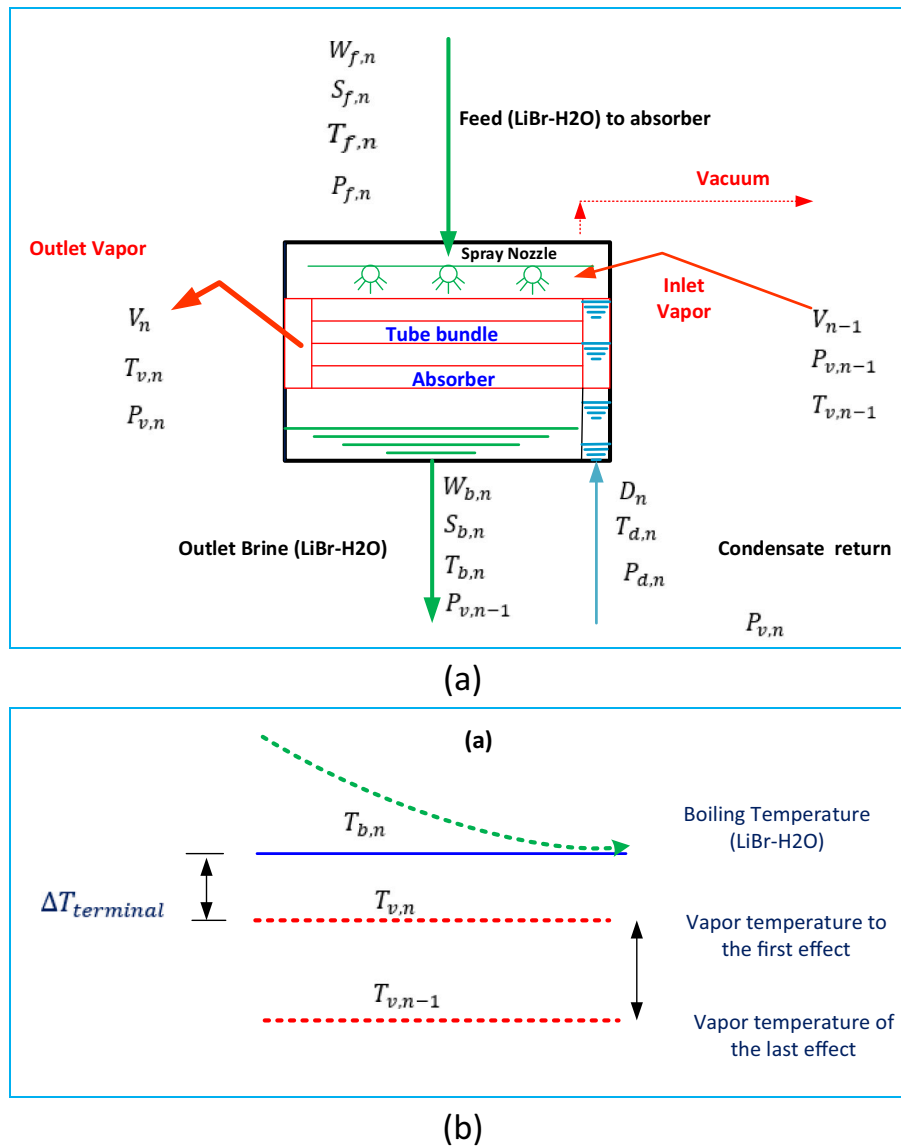


Fig. 8. Absorber; (a) Control volume and (b) Temperature distribution.

from the last effect of the evaporator, LiBr-H<sub>2</sub>O feed and distillate) and 2 outlet streams (generated steam in tube, LiBr-H<sub>2</sub>O brine outlet). Each stream is defined with its properties such as pure water flow rate, salt flow rate, temperature, and pressure. The number of unknowns is identified accordingly, and the number of governing equations is presented as follows:

Water balance for Absorber:

$$V_{n-1} + W_{f,n} + D_n = V_n + W_{b,n} \quad (17)$$

$$V_n = D_n \quad (18)$$

Salt balance for Absorber:

$$S_{f,n} = S_{b,n} \quad (19)$$

Heat balance around the Absorber:

$$V_{n-1}h_{v,n-1} + (W_{f,n} + S_{f,n})h_{LiBr-H2O,in} + D_n h_{d,n} = V_n h_{v,n} + (W_{b,n} + S_{b,n})h_{LiBr-H2O,out} \quad (20)$$

As shown in Fig. 8 ('a' and 'b'), the vapor ( $V_{n-1}$ ) of the last effect

absorbed by high concentrate LiBr-H<sub>2</sub>O solution, while the LiBr-H<sub>2</sub>O solution is sprayed on the outer the tubes until reach the equilibrium (boiling). Due to absorption (latent heat of condensed vapor into the solution), heat is liberated to boil the water inside the tubes and generates another vapor ( $V_n$ ). The equilibrium state is determined at the shell pressure ( $P_{v, n-1}$ ) and the salinity of the LiBr-H<sub>2</sub>O solution at inlet ( $X_{out}$ )

$$T_{boiling,Generator} = \phi(P_{v-1,n} \& X_{out}) \quad (21)$$

The temperature difference ( $\Delta T_{terminal}$ ) between the vapor ( $T_{v, n-1}$ ) and the LiBr-H<sub>2</sub>O fall ( $T_{b, n}$ ) is presented as

$$\Delta T_{terminal} = T_{b,n} - T_{v,n} \quad (22)$$

The terminal temperature ( $\Delta T_{terminal}$ ) is determined from heating load, the overall heat transfer coefficient ( $U$ ) and the heating surface area ( $A$ ) of the tube bundle:

$$V_{n-1}h_{v,n-1} - D_n h_{d,n} = UA\Delta T_{terminal} \quad (23)$$

The overall heat transfer ( $U$ ) in Eq. (24) is calculated as:

$$U = 1 / \left( \frac{1}{h_i} + \frac{1}{h_o} + \frac{t}{k} + FF \right) \quad (24)$$

And heat transfer area ( $A$ ),

$$A = n\pi DL \quad (25)$$

where,  $n$ ,  $D$  and  $L$  are related to tube number, diameter, and length, respectively.

Also, the pressure of the absorber ( $P_{boiling, absorber}$ ) is determined by the thermodynamic balance around the tube bundle of the absorber.

$$P_{boiling, absorber} - P_{b,n} = 0 \quad (26)$$

$$P_{b,n} - P_{v,n-1} = 0 \quad (27)$$

$$P_{v,n} - P_{D,n} = 0 \quad (28)$$

$$P_{f,n} - P_{b,n} = \varnothing(\Delta T_{subcooling}) \quad (29)$$

$$P_{v,n} = \text{specified} \quad (30)$$

Lithium Bromide – Water enthalpy (kJ) [15]:

$$h_{LiBr-water} = \sum_{n=0}^4 a_n x^n + T \sum_{n=0}^3 b_n x^n + T^3 d_0 \quad (31)$$

where,

$$a_0 = -954.8, a_1 = 47.7739, a_2 = -1.59235, a_3 = 2.09422 \times 10^{-2}, a_4 = -7.689 \times 10^{-5}$$

$$b_0 = -3.293 \times 10^{-1}, b_1 = 4.076 \times 10^{-2}, b_2 = -1.36 \times 10^{-5}, b_3 = -7.1366 \times 10^{-6}$$

$$c_0 = 7.4285 \times 10^{-3}, b_1 = -0.1544 \times 10^{-4}, b_2 = -1.3555 \times 10^{-6}$$

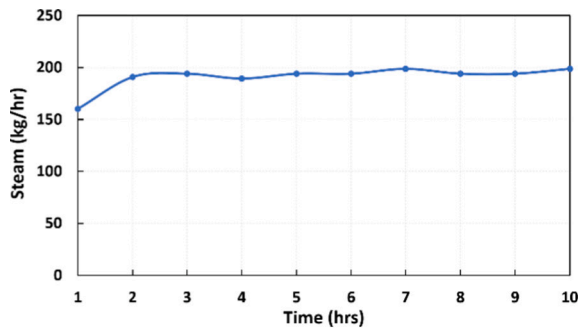
$$d_0 = -2.269 \times 10^{-6}$$

## 4. Results and discussion

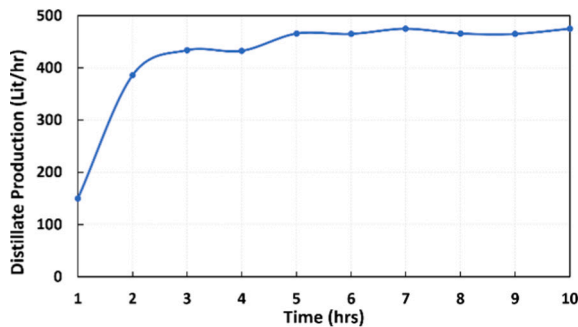
### 4.1. Pilot testing of MED-AB

A number of experiments have been carried out in the EVAP mode (i. e., standalone MED mode), with feed flowrates varying from 1 to 2.5 ton/h per cell and top brine temperature (TBT) of 65 °C. At seawater flowrate of 1.75 ton/h per cell, different experimental results are presented in Fig. 9. The commencement of steady state is defined as the time when the TBT of the first cell stabilizes to a fix value (65 °C in this case), along with the steam consumption and distillate production becoming consistent. The SCADA PLC algorithm is configured to maintain the set TBT of 65 °C by manipulating the steam input and the cooling reject flowrate, along with water-ejector aiding the release of non-condensable gases (NCGs). The online venting of the NCGs would avoid thermal resistance around heat transfer tubes. The experimental results show that the presence of even a small mole fraction of NCGs can deteriorate the heat transfer rate up to orders of magnitudes, almost quadratic under certain conditions [24].

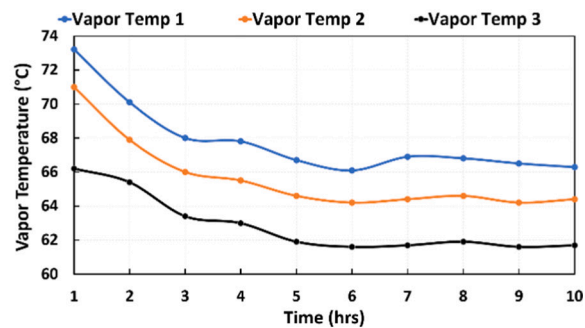
As can be seen in Fig. 9 (a) to (c), the system takes almost 5 h to reach steady state, where the control is based on the SCADA algorithm. Fig. 9 (a) presents the total average hourly steam consumption. As can be seen, the steam consumption is consistently around 195 kg/h (where the maximum steam producing capacity of the electrical boiler is 200 kg/h once the system reaches steady state). Similarly, Fig. 9 (b) presents the temperature profiles for the vapor generated in the three evaporator stages, where the temperature of the evaporator ('Vapor Temp 1') stabilizes to around 67.8 °C (where the given set point was 65 °C), after reaching the steady state. As can be seen from the trends of Fig. 9 (b), the vapor temperature differences between all of the three stages are approximately 2.5 °C or lower. The extraction timings of the generated NCGs were optimized manually by observing the behavior of the system. Fig. 9 (c) presents the total average hourly distillate production. As can be seen, the distillate production varies between 465 to 475 kg/h once the system reaches steady state. The salt rejection is shown in Fig. 9 (d),



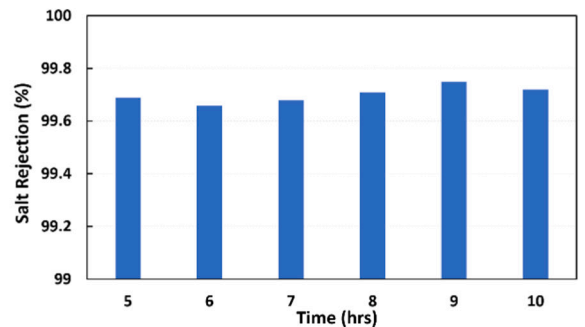
(a) Steam consumption



(c) Distillate production



(b) Vapor temperatures



(d) Salt rejection

Fig. 9. EVAP mode: Various experimental results at a feed flowrate of 1.75 ton/h per cell at a TBT of 65 °C.

where it is lower during the initial transient conditions, where the entrainment of the vapor with seawater/brine is higher due to unsteady and very dynamic conditions of the system. However, the salt rejection improves when the system approaches steady state operation and vapor velocity inside the evaporators becomes stable. The salt rejection calculated for 6 h of steady state operation is around 99.75%, which is acceptable under a high seawater feed salinity of 57,500 ppm (57.5 g/l). The average seawater temperature during this experiment was around 22.3 °C.

Similarly, a number of experiments have also been carried out in the FULL mode (i.e., integration of MED-AB), with feed flowrates varying from 1 to 2.5 ton/h per cell and top brine temperature (TBT) of 65 °C. As an example, for the flowrate of 1.75 ton/h/cell, different experimental results are presented in Fig. 10.

As can be seen in Fig. 10 (a) to (c), the system takes almost 5 h to reach steady state, where the control is based on the SCADA algorithm. As can be seen in Fig. 10 (a), the average steam consumption is consistently around 99.8 kg/h. From Fig. 10 (b) the temperature of the evaporator ('Vapor Temp 1') stabilizes to around 67.7 °C (where the given set point was 65 °C), after reaching the steady state. As shown in Fig. 10 (c), the performance ratio value evolving around average value 5.0 once the pilot plant reaches steady state. The salt rejection as shown in Fig. 10 (d) is again displayed from hour 5 onwards, when the system reaches steady state. Same as before, it is lower during the initial transient conditions and improves when the system approaches steady state operation. The salt rejection calculated for 6 h of steady state operation like before is around 99.75%. The average seawater temperature during this experiment was around 21.7 °C.

The performance ratio (or the gained output ratio) is defined as the ratio of distillate produced to the steam consumed. The experimental results, shown in Figs. 9 and 10, clearly suggest that at a same flow rate (1.75 ton/h per cell) and same TBT (65 °C), the steam consumption in case of FULL mode is less. From this, we can conclude that the FULL mode (i.e., integration of MED with AB) gives us a higher PR.

For verifying the repeatability of the experiments in the integrated MED-AB mode (i.e., FULL mode), the experiment at flowrate of 1.75 m<sup>3</sup>/

h per cell and at TBT of 65 °C (Fig. 11) was performed 4 times to observe and quantify the variation of the PR. As shown in Fig. 11, for the MED stand alone, the performance ratio values were recorded with little variation (6%) from the average. However, it is observed that, for full mode MED-AB, the variation in the recorded PR is about 22% which is due to the steady state in the MED-AB requires more time to match both MED and AB systems. The average PR of EVAP mode (MED) is around 2.7. The average PR of the MED-AB is around 3.8, which is 42% higher than that of the stand-alone MED, as shown in Fig. 11. This is owing to the recycling the vapor of the last stage and via AB system and used as heating steam to the first cell in addition to the extra steam which is generated within the absorber and used as heating steam to the first cell. This in turn reduces the amount of motive steam required from the boiler to almost half of the original value.

#### 4.2. Validation of the mathematical model

The previously developed and verified Visual Simulation Program (VSP) simulation code by Mabrouk et al. [22] will be subjected to further development to generate the code and solve the governing equations of the mathematical model of both absorber and generator. Fig. 12 shows the interface of the VSP simulator for the absorption/generator system (AB). The AB system has been adopted as vapor compressor.

Table 1 shows the design and operating parameters of the pilot plant which is specified as input to the VSP simulator. The vapor of the last effect (200 kg/h & 55 °C) is absorbed due to interaction with concentrated LiBr-Water feed (51%) around the tube bundle of the absorber. The equilibrium temperature (77 °C) has been reached at the shell pressure and the outlet LiBr-Water concentration (47%). Heat transferred from falling film around tubes is used to boil the inner pure water and get amount of vapor (200 kg/h & 71 °C) and directed to the first effect. The diluted LiBr-Water (47%) is directed to the generator via heat exchanger for preheating. In the generator, motive steam (216 kg/h & 106 °C) is used to generate second amount of vapor (200 kg/h & 67 °C) and the LiBr-Water get concentrated again to (51%). The generated vapor within the generator is mixed with that generated in the absorber

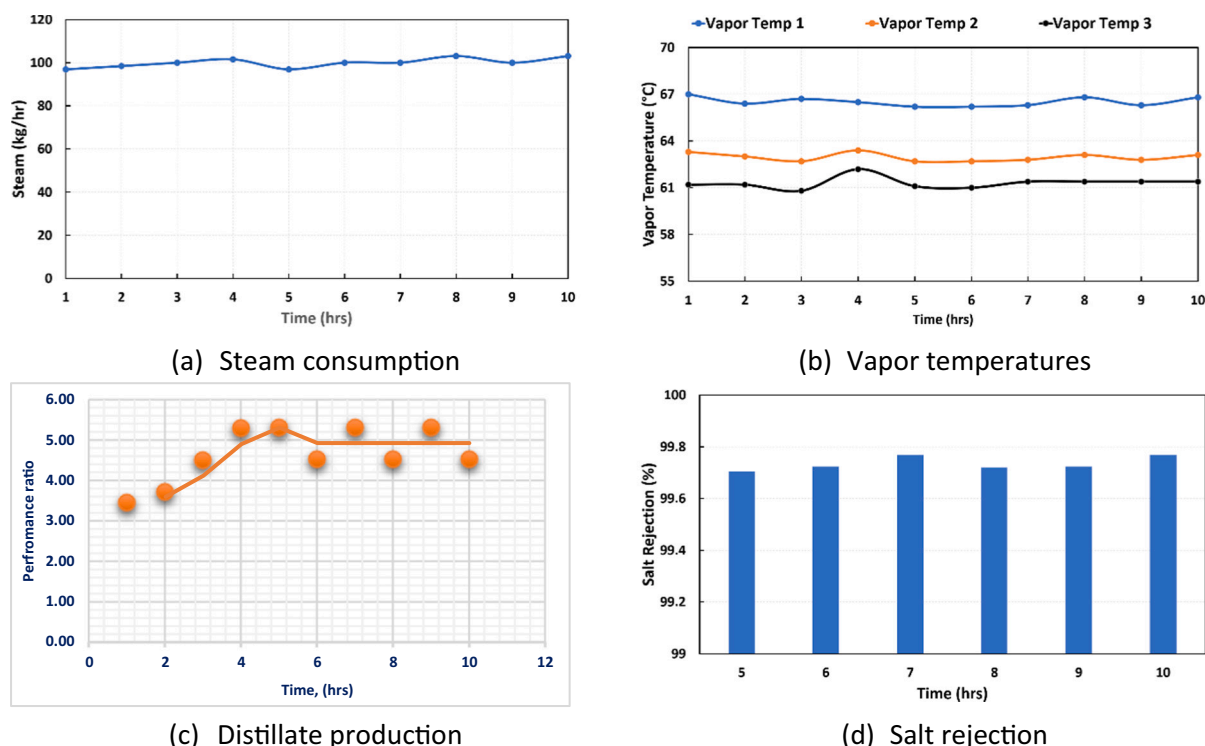


Fig. 10. FULL mode: Various experimental results at a feed flowrate of 1.75 ton/h per cell at a TBT of 65 °C.

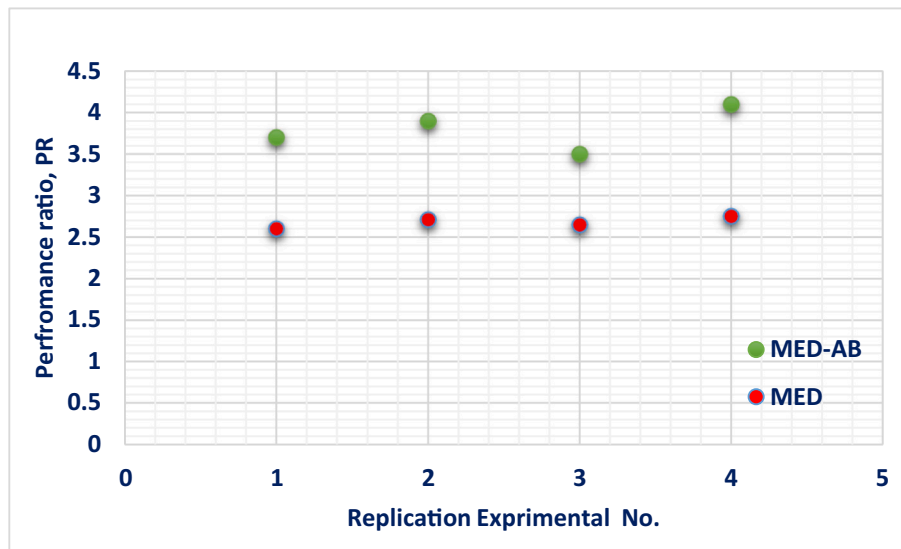


Fig. 11. Performance ratio comparison between ‘EVAP’ (MED) and ‘FULL’ (MED-AB) mode experiments at 1.75 ton/h per cell & TBT = 65 °C.

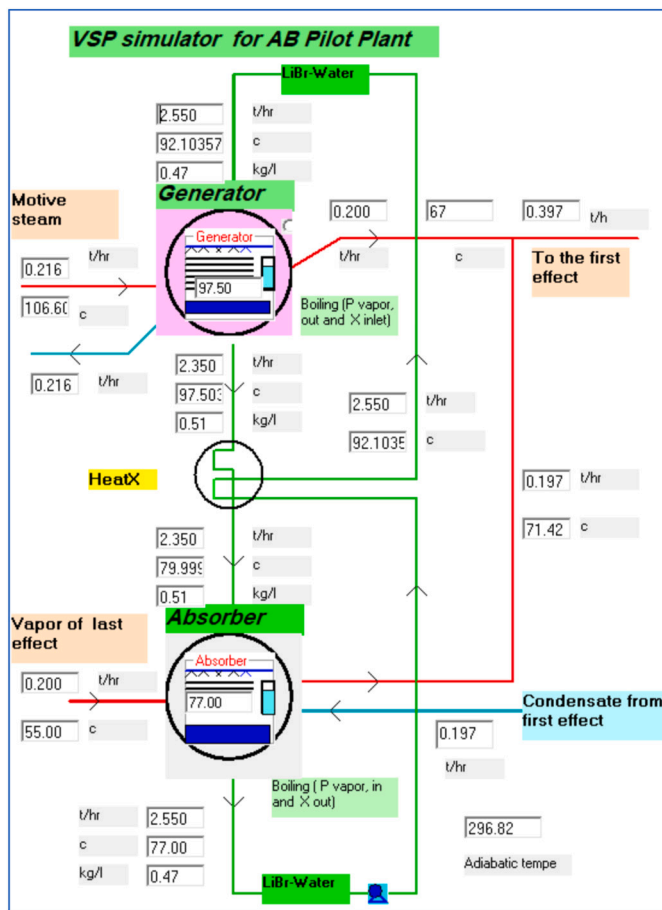


Fig. 12. VSP interface for simulation of the AB pilot plant.

and directed to first effect of the evaporator (400 kg/h & 68 °C). The concentrated LiBr-Water (51%) is circulated back to the absorber via heat exchanger.

Table 2 shows comparison between the simulation and the pilot plant results. The range of difference between measured and simulated varies is recorded to be ±8%, as shown in Table 1 which is in acceptable

Table 1

Input data to the VSP of the Absorber/Generator (AB) system.

AB pilot plant	Pilot test	Simulation	%diff
Boiler steam flow rate, kg/h	216	216	–
Boiler steam temperature, °C	106	106	–
LiBr-Water, inlet flow rate to absorber, kg/h	2350	2350	–
LiBr-Water, inlet flow rate to generator, kg/h	2550	2550	–
Vapor flow rate to absorber, kg/h	200	200	–
Vapor temperature to absorber, °C	55	55	–
Pure water to in tube absorber, kg/h	200	200	–
Generator heat transfer area, m <sup>2</sup>	20	20	–
Absorber heat transfer area, m <sup>2</sup>	20	20	–
Heat exchanger heat transfer area, m <sup>2</sup>	3.5	3.5	–

Table 2

Comparison between the pilot test and simulation of the Generator.

AB pilot plant	Pilot test	Simulation	%diff
LiBr-Water Concentration (inlet absorber), %	54	51	–6%
LiBr-Water Concentration (outlet absorber), %	49	47	–4%
Boiling temperature (Generator), °C	91	98	8%
Boiling temperature (absorber), °C	75	77	3%
Generated vapor temperature (absorber), °C	67	70	4%
Generated vapor temperature (generator), °C	66	67	2%
LiBr-Water temperature (inlet generator), °C	85	92	8%
LiBr-Water temperature to absorber, °C	77	80	4%

agreement between the simulation and pilot plant results.

Fig. 13 shows the interface of the VSP simulator of the integration of MED-AB pilot plant. Table 3 summarizes the input data of design and operating parameters to the VSP simulator. The boiler steam (216 kg/h & 106 °C) is specified to the generator, the seawater feed of 1750 kg/h & 55 g/l is specified for each effect, the pure water feed to the absorber in tube (200 kg/h). The heat transfer area is specified to each effect of (50 m<sup>2</sup>) the evaporator, the brine/feed plate heat exchanger (6 m<sup>2</sup>), the distillate/feed plate heat exchanger (2.5 m<sup>2</sup>), and condenser (18 m<sup>2</sup>), the absorber (20 m<sup>2</sup>) and the generator (20 m<sup>2</sup>). The sea water temperature of 35 °C and 8800 kg/h is specified, while part of it is directed to the condenser, while the rest is apportioned between brine/feed and distillate/feed heat exchangers. The VSP simulates the system under specified design and operating conditions to determine the production of 1006 kg/h at 36 °C, while the brine reject is 4180 kg/h at 41 °C, as shown in Fig. 13 and Table 4. The percentage difference between the

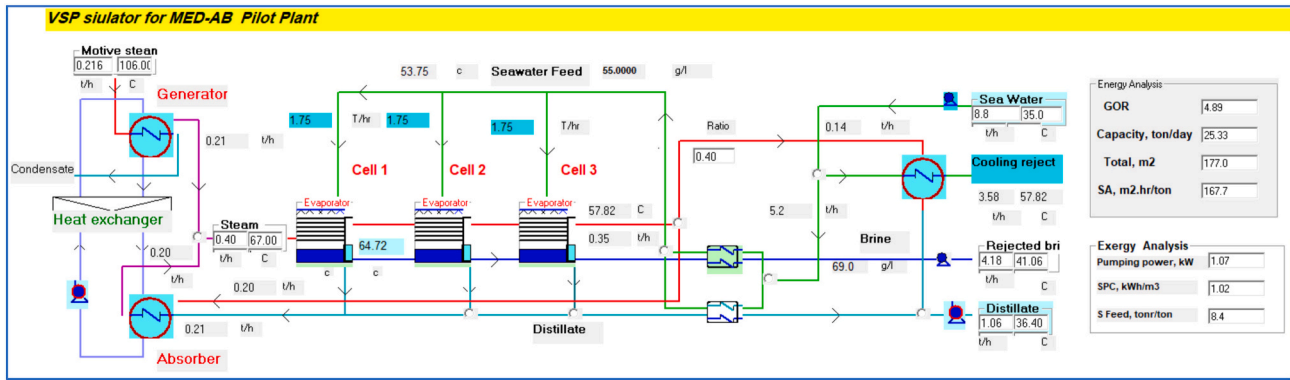


Fig. 13. Interface of the VSP simulator for the MED-AB pilot plant.

Table 3  
Specified data of the MED-AB pilot plant to the VSP.

Pilot plant (MED-AB)	Pilot test	Simulation	%diff
Evaporator surface area, m <sup>2</sup>	150	150	–
Brine heat exchanger, m <sup>2</sup>	6	6	–
Distillate heat exchanger, m <sup>2</sup>	2.5	2.5	–
Condenser	18	18	–
Absorber, m <sup>2</sup>	20	20	–
Generator, m <sup>2</sup>	20	20	–
Heat exchanger, m <sup>2</sup>	3.5	3.5	–
Cell 1, Seawater feed flow rate, kg/h	1750	1750	–
Cell 2, Seawater feed flow rate, kg/h	1750	1750	–
Cell 3, Seawater feed flow rate, kg/h	1750	1750	–
Boiler steam flow rate, kg/h	2016	2016	–
Boiler steam temperature, °C	106	106	–

Table 4  
Comparison between the pilot test and VSP simulation of the MED-AB.

Evaporator (MED)	Pilot test	Simulation	%diff
Cell 1, Vapor temperature, °C	62	63	2%
Cell 2, Vapor temperature, °C	59	60	2%
Cell 3, Vapor temperature, °C	55	57.8	5%
Brine flow rate, kg/h	4310	4180	–3%
Brine salinity, g/l	67	69	3%
Process recovery ratio, %	18	20	11%
Production, kg/h	940	1000	6%
Performance ratio (PR).	4.2	4.8	14%

VSP and pilot plant vapor temperature is about 2–5%. The difference is 3% in calculating the brine reject and brine salinity. The VSP simulator shows process recovery ratio is 11% higher than the pilot plant due to lower brine flow rate reject for the same input of seawater feed flow rate. There is 14% difference between VSP and the measured value of the performance ratio, as shown in Table 4. This difference is attributed to the ideal prediction of the model and the accuracy/uncertainty of the instrumentations measurement.

4.3. Technoeconomic analysis of commercial MED-TVC and MED-AB plants

An in-house developed Visual Simulation Program (VSP) code has been used to compare the proposed MED-AB technology with a commercial largest size unit evaporator MED-TVC plant (15 MIGD) installed in Saudi Arabia. The details of the VSP code development and its validation using the aforementioned commercial MED-TVC plant has already been detailed extensively in the earlier work of the authors [23]. Here we use the same VSP simulator to simulate the proposed MED-AB technology for large scale unit evaporator of 15 MIGD.

Fig. 14 illustrates a schematic diagram of the proposed MED-AB system for large scale desalination plant; a parallel feed multi effect distillation process of 10 cells driven by absorption vapor compressor (AB). The vapor from the last cell 10, stream No. 1, is routed to the absorber then absorbed by the concentrated LiBr-Water solution, stream No. 3. The absorption process is exothermic; the released thermal energy, which is utilized to generate vapor, stream No. 5. This vapor forms

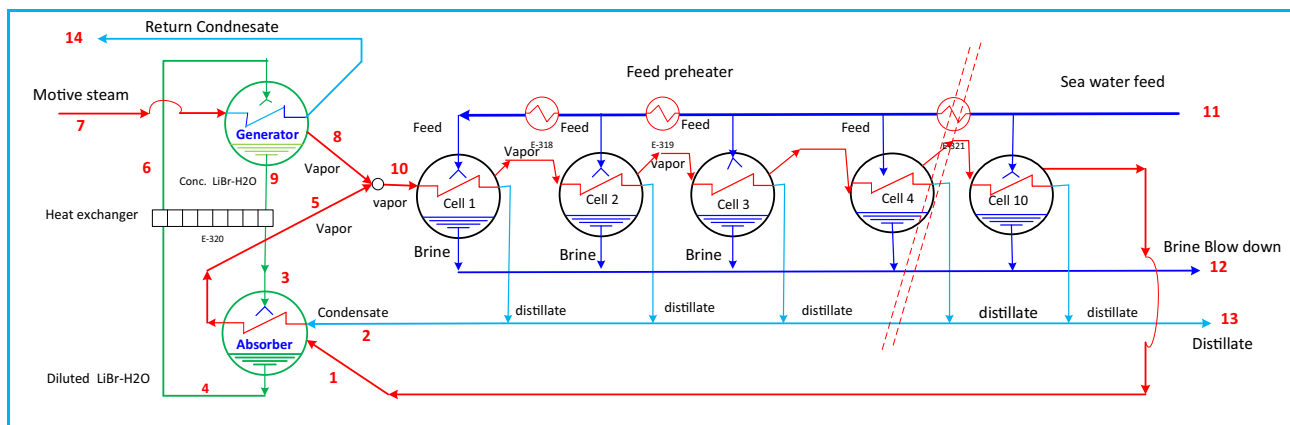


Fig. 14. Process flow diagram of the proposed MED-AB for large scale desalination plant.

part of the heating steam in the first effect of MED evaporator. The diluted LiBr-H<sub>2</sub>O solution, stream No. 4, exchanges heat with concentrated solution, stream No. 9, through heat exchanger before enters the generators. While the motive steam, stream No. 7, flows inside the tubes, the temperature of the LiBr-H<sub>2</sub>O solution increases to the saturation conditions and results in evaporating the same amount of water vapor absorbed by the solution in the absorber. The formed vapor in the generator, and absorber, stream No.10, is routed to the first cell (effect) of MED evaporator. Seawater feed, stream No. 11 is distributed in parallel.

Using the VSP and the specified process parameters as shown in Table 5, a comparison between the proposed novel MED-AB configurations is shown in Fig. 15 and the existing commercial MED-TVC (as shown in Fig. 16) has been performed. The conventional MED-TVC plant has only 7 effects, whereas in the present invention, with an improved evaporator design by minimizing the thermal losses would enable to accommodate a higher number in the same operating range, therefore we proposed 10 effects. The increase in the number of effects has a feature to increase the performance ratio, however the downside of it is that the heat transfer area also increases (CAPEX increase). Which explains that the heat transfer area of the novel design is 40% higher than that of the conventional design. This is due to employing 10 effects instead of 7 effects in the reference plant. But on the other hand, the reduction in the shell of the novel evaporator and reduction in the mechanical parts due to reduction in the intake/outfall facility would be equal to the increase of the heat transfer area. In this work, we aim to compromise between the slight increase in the capital cost and the substantial decrease in the OPEX due to the reduction in the energy consumption.

The heating steam of the conventional MED-TVC is 3 bar, however it is only 1 bar for the invention MED-AB, which indicates that a low-quality and low-price steam is used by the MED-AB. As shown in Table 5, for the same product capacity (15 MIGD), the performance ratio of the MED-TVC is 9, while it is 16 for the invention (MED-AB) (79% higher). This is because the heating steam flow rate of the conventional MED is 323 ton/h, while it is only 178 ton/h for the novel MED-AB. The intake feed flow rate of the MED-AB is 70% lower than the conventional MED-TVC due to the removal of the condenser. Accordingly, the pumping power of the invention is 55% lower than that of the conventional design. In this case, there is no need for cooling water which is usually 7–10 times of the production in the conventional MED plant.

The methodology of calculating the specific energy consumption for both MED-TVC and MED-AB is presented in Supplementary (A.6). The specific energy consumption (SEC) of the MED-AB is calculated as 4.8 kWh/ m<sup>3</sup>, which is 60% lower than the existing MED-TVC plant (13 kWh/ m<sup>3</sup>), as shown in Fig. 17.

The cost analysis of the commercial scale of MED-TVC and MED-AB are performed to calculate the unit water cost and compare using the same platform of VSP simulator. Table 6 shows a comparison between the capital investments of both configurations. The evaporator cost includes the tube cost, shell (host of the tube bundle), the internal

construction of the evaporator and evaporator steel structure above the foundation. The mechanical parts include circulation pumps, control/manual valves, fittings, piping and electrical/instrumentation and control. The capital investment also includes the construction of the intake/outfall of the seawater flow/ brine reject and the construction of large tank to desalinated water storage. The indirect capital investment includes relevant service such engineering, installation/ commissioning, and legal/ financial. The evaporator cost of the proposed MED-TVC is 16% higher due to the increase of the heat transfer area since MED-AB uses 10 cells, while the MED-TVC is restricted to 7 cells. The mechanical equipment of the present MED-AB is 16% lower than that of the traditional MED-TVC. This is mainly due to use small size for pumps, fittings, and piping due to removal of condenser with its control system. The capital investment of the intake/outfall work of the MED-AB process is 70% lower than that of the traditional MED-TVC due to elimination of rejected cooling water hence reducing the capacity of the outfall/discharge facilities. Table 6 indicates that the specific capital cost of the novel design (MED-AB) is the same of the conventional design (MED). This is attributed to the reduction of the capital cost of the intake/outfall civil work, mechanical parts in addition to the significant reduction of the shell material which compensates the increase of the heat transfer area of the tubes.

The OPEX analysis includes the cost of the required heating steam to drive the desalination unit, the electrical power cost of pumping, the cost of the chemicals, labor and insurance as shown in Table 6. The cost of electrical consumption is calculated using the specific electrical cost of 0.05 \$/kWh. Cost of the heating steam is calculated using the specific electrical cost of 0.05 \$/kWh and the calculated SEC of 13 and 5 kW for both configurations using the allocation method, as explained in the supplementary (A.6). The chemical cost including anti-scaling additives, anti-foam, chlorination is calculated based on recent commercial project. The specific operating cost (OPEX) of the MED-AB is 38% lower than the conventional MED. This is due to the 79% improvement in the performance ratio in addition to 55% reduction in the pumping power. The levelized unit water cost (over 25 years and with interest rates of 7%) of the invention is calculated as 0.455 \$/m<sup>3</sup>, which is 22% lower than that of the conventional MED-TVC desalination plant.

## 5. Conclusions

An advanced integrated Multi Effect Distillation with Absorption compressor (MED-AB) pilot plant has been installed based on an in-house design with a significant improvement to the traditional process. With a nominal capacity of 25 m<sup>3</sup>/day, the new MED-AB design has been validated under typical seawater salinity of 57,500 ppm (Dukhan, West coast of Qatar), operating at a top brine temperature (TBT) of 65 °C.

The conclusions of this work are summarized as follows:

1. The pilot plant results showed that the performance ratio of the MED-AB process is 42% higher than that of the MED. This is owing to the recycling of the vapor of the last stage via the AB system, in addition to the extra steam that has been generated within the absorber. This in turn reduces the amount of motive steam required from the boiler, almost to half of the original value.
2. The pilot plant AB results are used to validate the VSP model; the difference between measured value of the pilot plant results and the simulated varies is recorded  $\pm 8\%$ . For the overall MED-AB system, the percentage difference between the VSP simulation and pilot plant vapor temperature is about 2% - 5%, while the difference is 3% in calculating the brine reject and brine salinity. The VSP simulator shows that the process recovery ratio is 11% higher than the pilot plant due to lower brine flow rate reject for the same input seawater feed flow rate, while there is 14% difference in the performance ratio. The range of percentage difference between the pilot test and simulation is within acceptable range.

**Table 5**

Process parameters comparison between novel and the conventional design of the MED evaporator.

Performance analysis	Conventional (MED-TVC)	MED-AB (invention)
Unit capacity, MIGD	15	15
Number of effects	7	10
Motive steam flow rate, ton/h	323	178
Motive steam temperature, °C	140	97
Motive steam pressure, bar	3	1.0
Intake flow rate/ton of distillate	9.5	2.8 (-70%)
Heat transfer area, m <sup>2</sup> /ton/h	127	179 (40%)
Power consumption, kWh/m <sup>3</sup>	1.8	0.71 (-55%)
Performance Ratio (PR)	9	16 (79%)

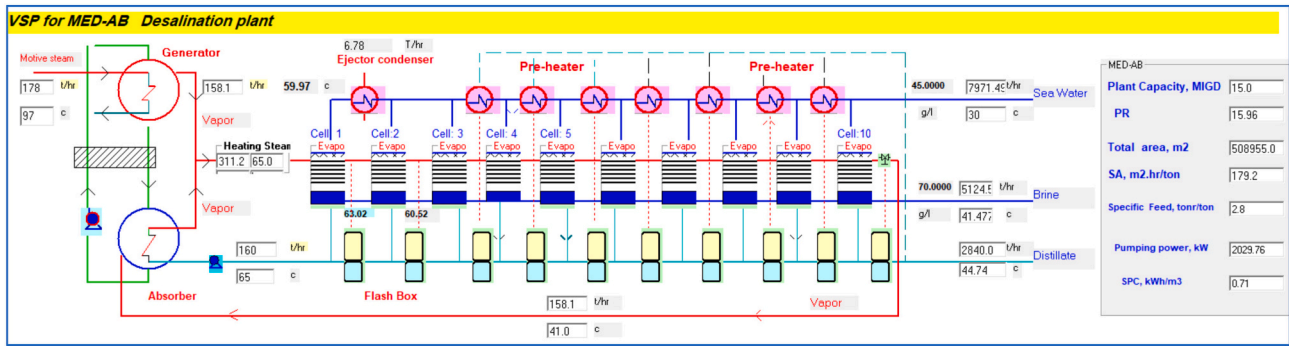


Fig. 15. VSP interface of the MED-AB for large scale, 15 MIGD desalination plant.

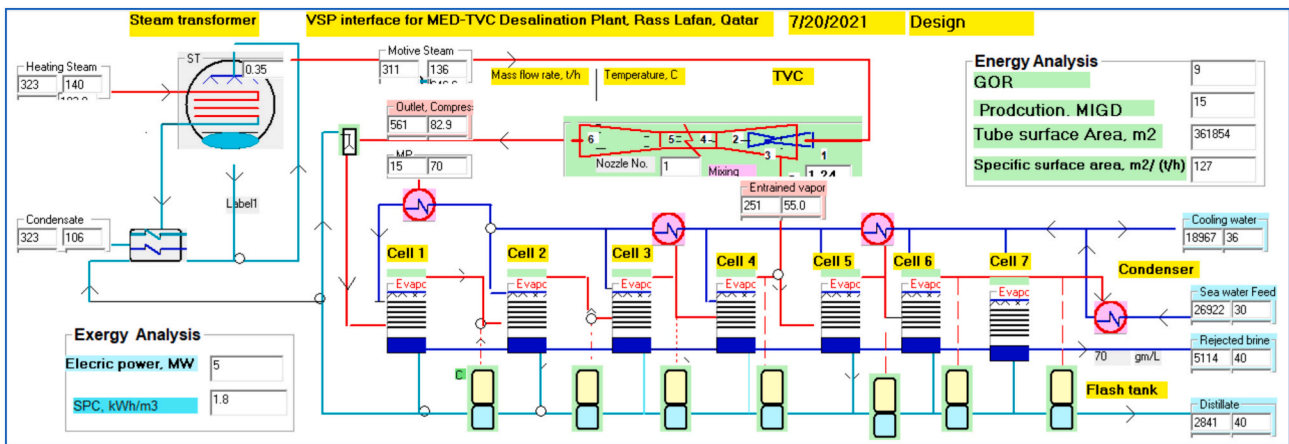


Fig. 16. VSP interface for the commercial MED-TVC, 15 MIGD (Saudi Arabia).

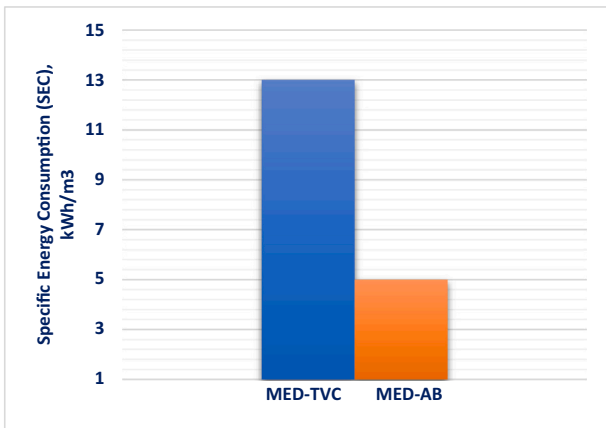


Fig. 17. Specific energy consumption for the invention (MED-AB) and MED-TVC plants.

3. The validated Visual Simulation Program (VSP) simulator has been used to compare the proposed MED-AB technology with a commercial largest size unit evaporator MED-TVC plant (15 MIGD), which has been installed in Saudi Arabia. The performance ratio of the commercial MED-TVC plant is 9, while it is 16 for the invention (MED-AB) (79% higher). This is because the heating steam flow rate of the conventional MED is 323 tons/h, while it is only 178 tons/h for the novel MED-AB. The intake feed flow rate of the MED-AB is 70% lower than the conventional MED-TVC due to the removal of the condenser. Accordingly, the pumping power of the invention is 55%

Table 6 Technoeconomic analysis of conventional and the novel MED design.

	MED-TVC	MED-AB	% diff
<b>Capital investment</b>			
Evaporator, \$	41,038,394	47,424,417	16%
Mechanical equipment, \$	7,968,710	6,677,269	-16%
Intakes, \$	7,753,420	2,295,790	-70%
Civil work, \$	9,136,656	9,133,440	0%
Potable water tank, \$	7,932,802	7,932,802	0%
Direct cost, \$	73,829,982	73,463,717	0%
Indirect cost, 25%, \$	18,457,496	18,403,200	0%
Total Capital, \$	92,239,662	91,866,917	0%
Specific CAPEX, \$/m <sup>3</sup>	0.246	0.245	0%
<b>Operation expenses</b>			
Steam, \$/h	194	36	-81%
Electricity, \$/h	241	33	-86%
Chemicals, \$/h	84	84	0%
Spare parts, \$/h	117	117	0%
Labor, \$/h	210	210	0%
Insurance, \$/h	117	117	0%
Total, \$/h	961.76	596.13	-38%
Specific OPEX, \$/m <sup>3</sup>	0.339	0.210	-38%
Levelized Water Cost, \$/m <sup>3</sup>	0.585	0.455	-22%

lower than that of the conventional design. The heat transfer area of the novel design is 40% higher than that of the conventional design. This is due to employing 10 effects instead of 7 effects in the reference plant.

4. An allocation method-based fuel energy consumption among combined cycle gas turbine (CCGT) power plant and (MED-TVC and MED-AB) desalination plant has been performed using the VSP simulator. The specific energy consumption (SEC) of the MED-AB is

calculated as 4.8 kWh/m<sup>3</sup>, which is 60% lower than the existing MED-TVC plant (13 kWh/m<sup>3</sup>).

- The cost analysis showed that the capital investment (CAPEX) of the novel design (MED-AB) is the same as that of the conventional design (MED). This is attributed to the reduction of the capital cost of the intake/outfall civil work, mechanical parts in addition to the significant reduction of the shell material which compensates the increase of the heat transfer area of the tubes. The specific operating cost (OPEX) of the MED-AB is 38% lower than the conventional MED. This is due to the 79% improvement in the performance ratio in addition to 55% reduction in the pumping power. The leveled unit water cost (over 25 years and with interest rates of 7%) of the invention is calculated as 0.455 \$/m<sup>3</sup>, which is 22% lower than that of the conventional MED-TVC desalination plant.

The advanced MED-AB technology has distinctive features which are summarized as below:

- Due to high performance MED-AB, the required seawater for condenser is minimized to zero, which in return minimize a huge amounts of thermal energy dumped back into the sea, that may affect marine life. The innovative solution not only saves on energy consumption, but also reduces the plant's capital investment, covering the feed pumps facilities, the intake/outfall civil work.
- The new tube arrangement that creates a new vapor route to eliminate the traditional demister which reduces the footprint and layout of the desalination plant and shell capital cost.
- Due to high performance of the novel MED-AB, this design would create a potential solution for the industrial application of high salinity byproduct and solar desalination.

## Declaration of competing interest

The authors declare that they have no known competing financial interests or personal relationships that could have appeared to influence the work reported in this paper.

## Acknowledgements

- To Qatar Environment and Energy Research Institute (QEERI), Water Center, Desalination Program RFP07 for granting internal fund to conduct this research including installation of the advanced MED pilot plant.
- To Qatar Electricity and Water Company (QEWC), as per 20-Year research collaboration agreement between QEWC and Qatar Environment and Energy Research Institute (QEERI). QEWC provided a building with all logistics (such as electricity, service water, full access to the seawater intake, and brine outfall facility) for installation of the Multi Effect Distillation (MED-AB) pilot plant. In this building we installed an advanced MED pilot plant and completed phase 1 of the project. Open Access funding provided by the Qatar National Library.

## Appendix A. Supplementary data

Supplementary data to this article can be found online at <https://doi.org/10.1016/j.desal.2021.115388>.

## References

- M. Mannan, M. Alhaj, A.N. Mabrouk, S.G. Al-Ghamdi, Examining the life-cycle environmental impacts of desalination: a case study in the state of Qatar, *Desalination* 452 (2019) 238–246, <https://doi.org/10.1016/j.desal.2018.11.017>.
- Global Water Intelligence (GWI), in: IDA Water Security Handbook 2020–2021, Media Analytics Ltd., Oxford, United Kingdom, 2020. <https://idadesal.org/e-libr ary/ida-water-security-handbook/>.

- S. Ihm, S. Woo, Comparative study on the methods of calculating theoretical minimum energy requirement for desalination, *Desalin. Water Treat.* 90 (2017) 32–45, <https://doi.org/10.5004/dwt.2017.21018>.
- A.N. Mabrouk, H.E.S. Fath, Technoeconomic study of a novel integrated thermal MSF–MED desalination technology, *Desalination* 371 (2015) 115–125, <https://doi.org/10.1016/j.desal.2015.05.025>.
- A.A. Mabrouk, K. Bourouni, H.K. Abdulrahim, M. Darwish, A.O. Sharif, Impacts of tube bundle arrangement and feed flow pattern on the scale formation in large capacity MED desalination plants, *Desalination* 357 (2015) 275–285, <https://doi.org/10.1016/j.desal.2014.11.028>.
- A. Mabrouk, A. Abotaleb, CFD analysis of the tube bundle orientation impact on the thermal losses and vapor uniformity within the MED desalination plant, *Desalin. Water Treat.* 143 (2019) 165–177, <https://doi.org/10.5004/dwt.2019.23558>.
- A. Abotaleb, A. Mabrouk, CFD analysis of the demister location impact on the thermal losses and the vapor uniformity within the MED desalination plant, *Desalin. Water Treat.* (2020), <https://doi.org/10.5004/dwt.2020.25222>.
- A. Abotaleb, A. Mabrouk, The impact of vapor box location on the performance of the multiple effect distillation for seawater desalination technology, *Desalin. Water Treat.* (2021), <https://doi.org/10.5004/dwt.2021.26821>.
- S. Ihm, O.Y. Al-Najdi, O.A. Hamed, G. Jun, H. Chung, Energy cost comparison between MSF, MED and SWRO: case studies for dual purpose plants, *Desalination* 397 (2016) 116–125, <https://doi.org/10.1016/j.desal.2016.06.029>.
- K.C. Ng, M. Burhan, Q. Chen, D. Ybyrayimkul, F.H. Akhtar, M. Kumja, R.W. Field, M.W. Shahzad, A thermodynamic platform for evaluating the energy efficiency of combined power generation and desalination plants, *Npj Clean Water.* 4 (2021) 25, <https://doi.org/10.1038/s41545-021-00114-5>.
- F.N. Alasfour, M.A. Darwish, A.O. Bin Amer, Thermal analysis of ME-TVC+MEE desalination systems, *Desalination* 174 (2005) 39–61, <https://doi.org/10.1016/j.desal.2004.08.039>.
- M.A. Darwish, A. Alsairafi, Technical comparison between TVC/MEB and MSF, *Desalination* 170 (2004) 223–239, <https://doi.org/10.1016/j.desal.2004.01.006>.
- Y. Wang, N. Lior, Thermoeconomic analysis of a low-temperature multi-effect thermal desalination system coupled with an absorption heat pump, *Energy* 36 (2011) 3878–3887, <https://doi.org/10.1016/j.energy.2010.09.028>.
- S.E. Aly, A study of a new thermal vapor compression/multi-effect stack (TVC/MES) low temperature distillation system, *Desalination* 103 (1995) 257–263, [https://doi.org/10.1016/0011-9164\(95\)00078-X](https://doi.org/10.1016/0011-9164(95)00078-X).
- I. Janghorban Esfahani, Y.T. Kang, C. Yoo, A high efficient combined multi-effect evaporation–absorption heat pump and vapor-compression refrigeration part 1: energy and economic modeling and analysis, *Energy* 75 (2014) 312–326, <https://doi.org/10.1016/j.energy.2014.07.081>.
- D.C. Alarcón-Padilla, L. García-Rodríguez, J. Blanco-Gálvez, Assessment of an absorption heat pump coupled to a multi-effect distillation unit within AQUASOL project, *Desalination* 212 (2007) 303–310, <https://doi.org/10.1016/j.desal.2006.10.015>.
- D.C. Alarcón-Padilla, L. García-Rodríguez, J. Blanco-Gálvez, Design recommendations for a multi-effect distillation plant connected to a double-effect absorption heat pump: a solar desalination case study, *Desalination* 262 (2010) 11–14, <https://doi.org/10.1016/j.desal.2010.04.064>.
- J. Su, W. Han, H. Jin, A new seawater desalination system combined with double-effect absorption heat pump, *J. Eng. Thermophys.* 29 (2008) 377.
- H. Rostamzadeh, H. Ghiasirad, M. Amidpour, Y. Amidpour, Performance enhancement of a conventional multi-effect desalination (MED) system by heat pump cycles, *Desalination* 477 (2020), 114261, <https://doi.org/10.1016/j.desal.2019.114261>.
- A. Mabrouk, Multi Effect Distillation Evaporator, 2016–31325, 2016.
- A.N. Mabrouk, H. Abdulrahim, *Desalination System*, 2017–32908, 2017.
- A.S. Nafey, H.E.S. Fath, A.A. Mabrouk, A new visual package for design and simulation of desalination processes, *Desalination* 194 (2006) 281–296, <https://doi.org/10.1016/j.desal.2005.09.032>.
- S. Aly, H. Manzoor, A. Abotaleb, J. Lawler, A. Mabrouk, Pilot testing of a novel multi effect distillation (MED) for seawater desalination technology, *Desalination* 519 (2021), <https://doi.org/10.1016/j.desal.2021.115221>.
- C.W. Lee, J.S. Yoo, H.K. Cho, Multi-scale simulation of wall film condensation in the presence of non-condensable gases using heat structure-coupled CFD and system analysis codes, *Nucl. Eng. Technol.* (2021), <https://doi.org/10.1016/j.net.2021.03.001>.

**Abdel Nasser Mabrouk** is a Senior Scientist at the water center, Qatar Environment, and Energy Research Institute (QEERI). Since 2014, he has been leading research in desalination technology development from the prototype to the pilot plant with a key focus on the realization of novel ideas to reduce energy consumption and reduce water unit cost. He is currently leading advances in thermal desalination in particularly, he built an advanced MED pilot plant with nominal capacity 25 m<sup>3</sup>/day based novel ideas to reduce energy consumption by 40% and reduce unit water cost by 30%. The pilot plant is running under high seawater salinity (57,000 mg/l) in direct collaboration with Qatar Electricity and Water Co. (QEWC), Qatar. He is also leading international consortia with industry and academic partnerships for fabrication of a novel thermoplastic heat exchanger for MED desalination, and using novel antiscalants, with funding from QNRF and HBKU, along with significant industrial cost-sharing. He holds a technical advisory role to Um Al-Houl Power and Desalination Plant, Qatar. Since 2017, he is jointly appointed to the College of Science and Engineering, HBKU, where he is teaching desalination technology and scientific advisory of MSc/PhD students.

Dr. Abdel-Nasser previously worked in the Desalination R&D Center, Doosan Heavy Industries Co., (2007–2014, South Korea, UAE and KSA) to develop a technical solution for

the commercial desalination plants in the GCC countries including Multi Stage Flash (MSF), Multi Effect Distillation (MED), and Reverse Osmosis (RO); leading a pilot plant program (MED, South Korea and MSF-OT, in KSA).

Dr. Abdel-Nasser graduated with a B.Sc. (1993, distinction with honor) in Mechanical Engineering, Alexandria University, Egypt, M.Sc. (1999) in Solar Desalination and PhD

(2006) in thermoeconomic of desalination process using visual simulation program, Suez University, Egypt, where he also served as Associate Professor prior to joining QEERI. He has participated in several European Commission funded projects in Solar Desalination, and has published 49 journal papers, 46 conference papers, 1 book and 2 book chapters. He has filed 4 GCC patent-pending, 1 PCT patent, and 2 US provisional patents.